Cobalt(II) Chloride Complex of Propylene-1,3-diamine as CO₂ Absorber

E. Liu and Fangfang Jian[*]

School of Chemical Engineering and Pharmaceutics, Henan University of Science and Technology, Luoyang, Henan Province, P.R. China

*Corresponding author: E-mail: ffj2013@163.com; 798233443@haust.edu.cn

A new CO_2 absorber is reported in this paper. When $CoCl_3$ is mixed with propylenediamine at room temperature and atmospheric ambient pressure, the extremely low concentration of CO_2 in the air can be absorbed to form a stable metal complex $[Co(PPD)_2CO_3]Cl \cdot H_2O$ (PPD = 1,3-propylenediamine). The CO_2 capture capacity can reach 23.6 wt. %. Although Co is relatively expensive, the practical use of cobalt metal complexes produced still needs to be developed. This study provides an idea of capturing CO_2 at low concentration under normal conditions. Through the structural characterization and performance study of complex $[Co(PPD)_2CO_3]Cl \cdot H_2O$, a new method for CO_2 capture was explored. Thermogravimetric analysis data show that the compound $[Co(PPD)_2CO_3]Cl \cdot H_2O$ has the ability to desorption CO_2 and H_2O at 160-220 ℃, and the ability to adsorb CO_2 or regenerate CO_2 is being explored. The electrochemical property of compound $[Co(PPD)_2CO_3]Cl \cdot H_2O$ were also investigated.

Keywords: Cobalt, 1,3-Propylenediamine, CO₂ absorber, Crystal structure, Electrochemistry.

INTRODUCTION

The huge amount of carbon dioxide emissions into the atmosphere due to the world′s fossil fuel utilization has led to an intensive amount of efforts to find effective procedures to reduce this greenhouse gas in the atmosphere [1-3]. The development of sustainable synthetic routes exploiting carbon dioxide as a largely available, cost effective and non-toxic synthon represents one of the most intriguing challenges for contemporary chemistry research [4,5]. Processes converting CO_2 into a range of useful chemicals have witnessed significant progress in the last decade [6,7]. Amine-based processes are the most mature carbon capture technologies for post-combustion CO_2 [8]. However, these processes have some drawbacks that make the substitution study more meaningful: high energy demand, volatility, corrosion, thermal stability and chemical stability are the most relevant adverse factors. Therefore, absorption technology, which makes CO_2 form stable compounds at room temperature and pressure, has become a research hotspot [9,10].

Chemical absorption may be the most applicable technology used to capture CO_2 from power plants. Due to the designable structure, unusual flexibility and precoordinated functional groups of metal complexes, porous materials of metal complexes have become more and more attractive. The cobalt complex *viz.*, $[Co(en)_3]Cl_3$, (en = ethylenediamine) is one of the most basic complexes in coordination chemistry [11,12]. In the synthesis of optically active or chiral complexes, it is often used as a template to prepare metal phosphate chiral frame materials [13,14]. The cobalt complex $[Co(en)_3]Cl_3$ has a property of gas adsorption, it contains water molecules in its one-dimensional channel [15-17]. In the study of $Co(PPD)Cl_3$ compound, (PPD = 1,3-propylenediamine), PPD is used instead of ethylenediamine, and obtained the unusual crystal structure of $[Co(PPD)_2CO_3]Cl \cdot H_2O$. It is sure that no carbonates were added or touched, so that the introduction of CO_3^{2-} anion shall be come from CO_2 in the atmosphere. It indicates that the mixture of 1,3-propylenediamine and $CoCl_3$ can absorb CO_2 gas to form stable compound under normal temperature and pressure. Although it is not economical to capture atmospheric CO_2 with precious cobalt metal, it is of scientific significance as a new way of CO_2 capture. In this paper, we reported, a crystal structure of compound $[Co(PPD)_2CO_3]Cl \cdot H_2O$ and thermogravimetric analysis and electrochemical study were also reported.

EXPERIMENTAL

1,3-Propylenediamine (PPD), $CoCl_3 \cdot 6H_2O$, ethanol, *etc*. are all analytical grade, without further purification and use as such.

Synthesis: The solid $CoCl_3 \cdot 6H_2O$ (2.75 g, 0.01 mol) was added to 1,3-propylenediamine (2 mL, 0.025 mol) containing stirring magneton, which was vigorously stirred and found pH value are changing to 5-6. Also, the mother solution change to the magenta transparent solution. The mother liquor was left to volatilize naturally to obtain red crystals suitable for X-ray diffraction analysis. Elemental analysis (found) %: C: 26.03; H: 7.05; N: 17.22. UV spectra: 350 nm is Co^{3+} charge shift transition, 520 nm is Co^{3+} $d{\to}d$ transition. IR (KBr, v_{max}, cm^{-1}): 3455, 3259 (N-H *str.*), 3215, 3122 (O-H *str.*), 1470-1400 (CO_3^{2-}), 1278, 1185, 1160 (C-N *str.*), 800-600 (M-Cl).

Detection method: Elemental analyses were measured with a Perkin-Elmer 1400C analyzer. Infrared spectra were recorded on a Nicolet 170SX spectrometer using pressed KBr plates in the 4000-500 cm^{-1} ranges. Thermogravimetry (TG) and differential thermal gravimetric (DTG) analyses were recorded on Netzsch-geratebau GmbH thermogravimetric analyzer for the crystalline samples under a nitrogen atmosphere (150 mL/min) at a heating rate of 20 ℃/min. The phase and purity of as-prepared products were determined by X-ray diffraction (XRD) and performed on a D/max-2500 X-ray diffractometer equipped with graphite monochromatized Cu$K\alpha$ radiation (λ = 1.5406 Å). Melting point was measured using WRR melting point meter; UV spectra was detected by CARY 50 UV spectrometer. Electrochemical properties are done by using the Autolab PGSTAT-30 electrochemical workstation, using three electrode system. The Au electrode is as working electrode, Pt slices (0.8 cm × 0.8 cm) as auxiliary electrodes, Ag/AgCl electrode as the reference electrode. All the potential measurements to electrode (236.3 mV, 20 ℃) as a reference ones.

Crystallographic data collection: The diffraction data were collected on a SMART APEXII diffractometer with graphite monchromatic Mo-$K\alpha$ (λ = 0.71073 Å, T = 293 K) radiation. Empirical absorption correction was carried out by using the SADABS program. Their structures were solved by direct methods and refined by least squares on $Fobs^2$ with SHELXTL software package. All non-H atoms were anisotropically refined. The hydrogen atoms were located by difference synthesis and refined isotropically. The molecular graphics were plotted using SHELXTL. Atomic scattering factors and anomalous dispersion corrections were taken from International data for X-ray crystallography. A summary of key crystallographic information is given in Table-1. Bond lengths and angles are given in Table-2.

RESULTS AND DISCUSSION

Single crystal X-ray diffraction studies: The crystal lattice of compound $[Co(PPD)_2CO_3]Cl \cdot H_2O$ is made up of host $[Co(PPD)_2CO_3]^+$ group, Cl^- anion and one H_2O molecule (Fig. 1). Co^{3+} lie in distorted octahedral coordination environment, with Co-N bond length of 1.965(2)~1.974(2) Å and Co-O that of 1.928(2) Å and 1.945(2) Å. These data are little different with the previous report of Zhu and Chen [18]. Cell parameters and space groups are completely different. The difference is probably due to that the compouns are isomers, moreover, present synthetic method is aslo different. The introduction of carbonate anions is caused by the absorption of extremely low concentrations of CO_2 in air.

TABLE-1
CRYSTAL DATA AND STRUCTURE REFINEMENT DETAILS FOR $[Co(PPD)_2CO_3]Cl \cdot H_2O$

Empirical formula	$C_7H_{22}N_4O_4ClCo$
Formula weight	320.66
Temperature	273(2) K
Wavelength	0.71073 Å
Crystal system	Monoclinic
Space group	P121/c1
Unit cell dimensions	a = 9.1450(18) Å
	b = 6.9010(14) Å
	c = 23.169(6) Å
Volume	1360.4(6) Å^3
Z	4
Density (calculated)	1.566 Mg/m^3
Absorption coefficient	1.467 mm^{-1}
F(000)	672
Crystal size	0.25 × 0.23 × 0.15 mm^3
Theta range for data collection	1.889 to 26.970°.
Index ranges	0<=h<=10, -8<=k<=0, -29<=l<=25
Reflections collected	3082
Independent reflections	2902 [R(int) = 0.0492]
Completeness to theta = 25.242°	100.0 %
Absorption correction	None
Refinement method	Full-matrix least-squares on F^2
Data/restraints/parameters	2902/0/154
Goodness-of-fit on F^2	1.054
Final R indices [I>2σ(I)]	R1 = 0.0413, wR2 = 0.1050
R indices (all data)	R1 = 0.0611, wR2 = 0.1138
Extinction coefficient	n/a
Largest diff. peak and hole	1.251 and -0.531 e.Å^{-3}

TABLE-2
SELECTED BOND LENGTH (Å) AND ANGLES (°)

Bond	Length (Å)	Bond	Length (Å)
Co1-O1	1.945(2)	O1-C7	1.309(4)
Co1-O2	1.928(2)	O2-C7	1.320(4)
Co1-N1	1.974(2)	O3-C7	1.247(4)
Co1-N2	1.971(2)	N1-C1	1.497(4)
Co1-N3	1.972(2)	N2-C3	1.491(4)
Co1-N4	1.965(2)	N3-C4	1.486(4)
Co1-C7	2.352(3)	N4-C6	1.484(4)
Bond angle	**Angle (°)**	**Bond angle**	**Angle (°)**
O1-Co1-N1	90.55(10)	O2-Co1-N4	166.12(9)
O1-Co1-N2	166.76(10)	O2-Co1-C7	34.12(9)
O1-Co1-N3	90.99(10)	N1-Co1-C7	91.43(10)
O1-Co1-N4	98.25(9)	N2-Co1-N1	89.47(11)
O1-Co1-C7	33.80(9)	N2-Co1-N3	89.00(10)
O2-Co1-O1	67.88(9)	N2-Co1-C7	132.96(11)
O2-Co1-N1	89.82(10)	N3-Co1-N1	178.45(10)
O2-Co1-N2	98.88(10)	N3-Co1-C7	89.77(10)
O2-Co1-N3	90.64(10)	N4-Co1-N1	91.08(11)
N4-Co1-N3	88.84(10)	N4-Co1-C7	132.00(10)

There is a number of hydrogen bonding in the crystal structure (Table-3). O_w-H⋯O distance of 2.904(4) Å is the longer than that of ice Ih (average 2.74Å), shows weak hydrogen bonding interaction [19]. The N-H⋯Cl hydrogen bonding interactions connect adjacent $[Co(PPD)_2CO_3]$ group to form a 1-D chain structure (Fig. 2), and then forms a 2-D network structure through N-H⋯O hydrogen bonding (Fig. 3). It shows that hydrogen bonding interactions play an important role in the stability of crystal structure.
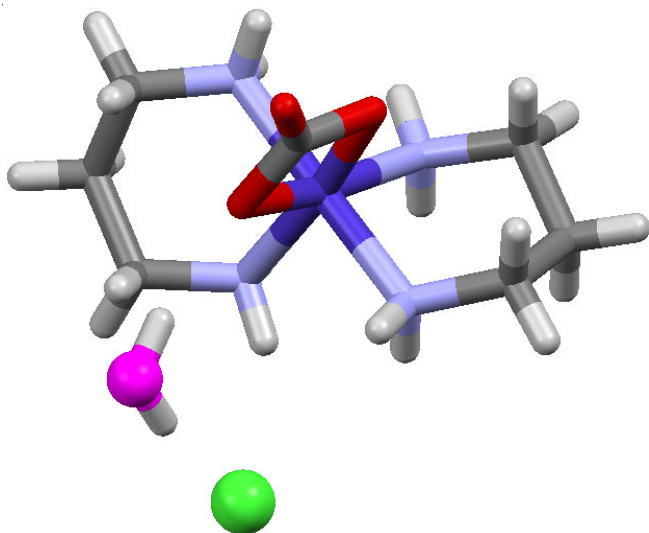
Fig. 1. Molecular structure of $[Co(PPD)_2CO_3]Cl \cdot H_2O$

TABLE-3
HYDROGEN-BOND GEOMETRY (Å, °)
FOR $[Co(PPD)_2CO_3]Cl \cdot H_2O$

Donor-H···Acceptor	D-H	H···A	D···A	D-H···A
N1-H1A···Cl1#1	0.89	2.62	3.392(3)	145.2
N2-H2A···Cl1#2	0.89	2.39	3.263(3)	166.4
N2-H2B···O3#3	0.89	2.34	3.038(4)	134.9
N3-H3A···O2#4	0.89	2.04	2.908(3)	166.5
N3-H3B···O3#3	0.89	2.08	2.967(3)	172.2
N4-H4A···Cl1#2	0.89	2.76	3.278(3)	118.6
N4-H4B···Cl1	0.89	2.44	3.245(3)	150.9
O1W-H1WA···O1	0.85	2.07	2.904(4)	165.5
O1W-H1WB···Cl1	0.85	2.49	3.310(4)	162.7

Symmetry transformations used to generate equivalent atoms: #1 -x,y-1/2,-z-1/2 #2 -x,y+1/2,-z-1/2 #3 x,y+1,z #4 -x+1,-y-1,-z
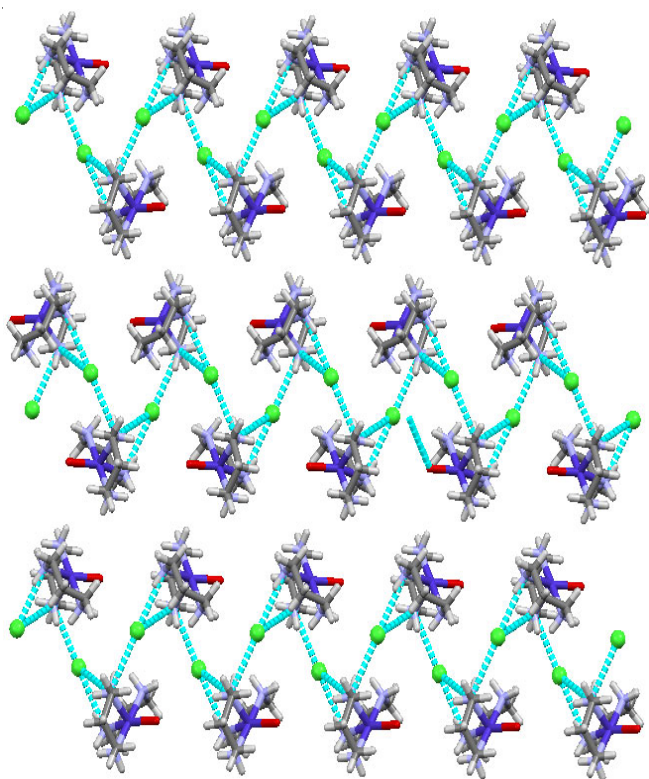

Fig. 2. N-H···Cl hydrogen bonding interactions

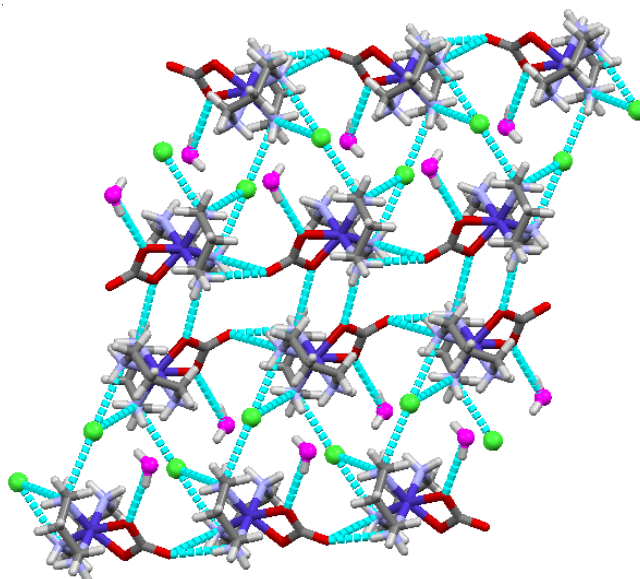Fig. 3. Two-dimensional network structure through hydrogen bonding

Thermal analysis: Thermograms of $[Co(PPD)_2CO_3]Cl \cdot H_2O$ complex are shown in Fig. 4. It can be observed that the decomposition of compound $[Co(PPD)_2CO_3]Cl \cdot H_2O$ accompanying by three key weight-loss processes, and with the three intense and two weak exothermal peak, respectively. During the first step of weight-lost process, there is a small sharp exothermal peak at 166.6 °C and the weight-lost is 5.73 %, which is assigned to lost H_2O molecule (calcd. 5.61 %). After 180 °C, the compound occurs to the second time decompose corresponding to another strong exothermal peak at 203.0 °C and loses weight 18.6 %, which is assigned to lost CO_3^{2-} (calcd. 18.71 %). Then, there are intense endothermic peak at 251.8 °C and two weak endothermic peaks at 334.8 and 390.9 °C, and the total weight loss of 44.02 % suggests that two propylene diamine molecules lost (calcd. 46.15 %). Finally, there is one broad hump in 500-700 °C temperature region and a very small endothermic peak at 603.3 °C and the weight loss of 9.66 % at 700 °C suggests that the residue should be Co (found 21.99 % calcd. 18.38 %).
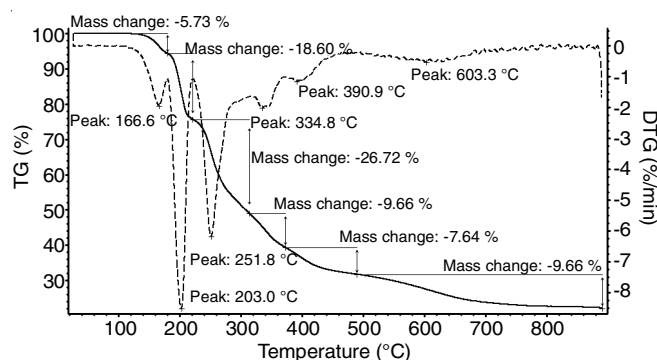
Fig. 4. Thermal analysis curve of $[Co(PPD)_2CO_3]Cl \cdot H_2O$

Electrochemical properties: Water was used as the solvent, 0.1 mol L⁻¹ (tetrabutyl ammonium perchlorate) (TBAP) as the supporting electrolyte and the complex concentration was 1.0 × 10⁻⁴ mol L⁻¹. Scanning was performed in the range of 0.5 ~ 1.6 V and cyclic voltammetry was used to study under room temperature anaerobic conditions. Fig. 5 is the cyclic voltammo-
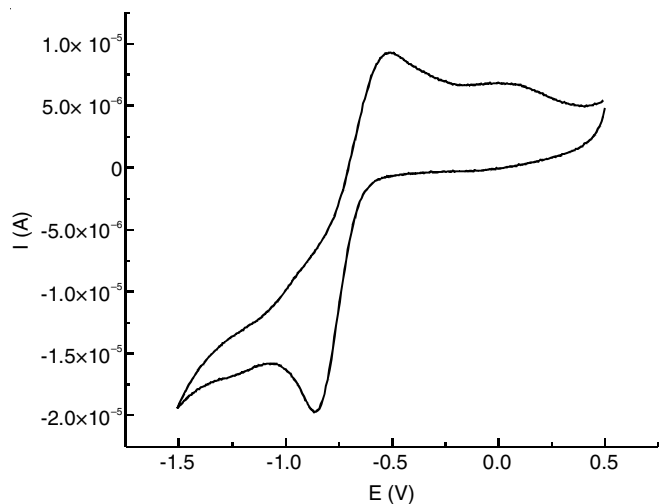
Fig. 5. Cyclic voltammograms of the complex [Co(PPD)$_2$CO$_3$]Cl·H$_2$O in aqueous solution containing 0.1 M TBAP at a scan rate of 0.05 V/s

gram of complex [Co(PPD)$_2$CO$_3$]Cl·H$_2$O. From the cyclic voltammogram, it can be seen that when the scanning rate is 0.05 v/s, there is a pair of redox peaks at -0.508 and -0.865 V. According to $\Delta E_p = E_{pa} - E_{pc} = 0.375$ V, and formula $E_o' = +E_{pa}(E_{pc})/2$, the calculation of electric potential (E_o') is 0.687 V, the cathode and anode as the potential difference of $\Delta E = 0.687$ V, $i_{pa}/i_{pc} = 1.51$, indicate that the complexes on the gold electrode electrochemical behaviour is not reversible redox process.

Conclusion

In this paper, a CO$_2$ absorber *viz.* [Co(PPD)$_2$CO$_3$]Cl·H$_2$O from air under normal temperature and pressure is developed. The mixture of propylenediamine and cobalt chloride can absorb the extremely low concentration of carbon dioxide gas in the air to form a stable compound [Co(PPD)$_2$CO$_3$]Cl· H$_2$O. The crystal structure analysis of compound shows that CO$_3^{2-}$ and H$_2$O can form strong hydrogen bond interaction, and the cobalt metal atoms form octahedral coordination environment with propylenediamine and carbonate, and chloride ion only acts as the balance charge. Thermogravimetric analysis showed that the compound may have the function of adsorption and desorption of CO$_2$ and further research is in progress.

CONFLICT OF INTEREST

The authors declare that there is no conflict of interests regarding the publication of this article.

REFERENCES

1. M. Ghahramaninezhad, B. Soleimani and M. Niknam Shahrak, *New J. Chem.*, **42**, 4639 (2018);
    https://doi.org/10.1039/C8NJ00274F.
2. S. Iglauer, *Int. J. Greenh. Gas Control*, **77**, 82 (2018);
    https://doi.org/10.1016/j.ijggc.2018.07.009.
3. H. Chen, T.C. Tsai and C.S. Tan, *Int. J. Greenh. Gas Control*, **79**, 127 (2018);
    https://doi.org/10.1016/j.ijggc.2018.10.002.
4. M. Aresta, *Coord. Chem. Rev.*, **334**, 150 (2017);
    https://doi.org/10.1016/j.ccr.2016.06.004.
5. A.W. Kleij, M. North and A. Urakawa, *ChemSusChem*, **10**, 1036 (2017);
    https://doi.org/10.1002/cssc.201700218.
6. M. Aresta, A. Dibenedetto and A. Angelini, *Chem. Rev.*, **114**, 1709 (2014);
    https://doi.org/10.1021/cr4002758.
7. P. Gao, S. Dang, S. Li, X. Bu, Z. Liu, M. Qiu, C. Yang, H. Wang, L. Zhong, Y. Han, Q. Liu, W. Wei and Y. Sun, *ACS Catal.*, **8**, 571 (2018);
    https://doi.org/10.1021/acscatal.7b02649.
8. J. de Riva, V. Ferro, C. Moya, M.A. Stadtherr, J.F. Brennecke and J. Palomar, *Int. J. Greenh. Gas Control*, **78**, 94 (2018);
    https://doi.org/10.1016/j.ijggc.2018.07.016.
9. I. Bauer and H.J. Knolker, *Chem. Rev.*, **115**, 3170 (2015);
    https://doi.org/10.1021/cr500425u.
10. X. Liu, S. Zhang, Q.W. Song, X.F. Liu, R. Ma and L.N. He, *Green Chem.*, **18**, 2871 (2016);
    https://doi.org/10.1039/C5GC02761F.
11. O.M. Yaghi, M. O'Keeffe, N.M. Ockwig, H.K. Chae, M. Eddaoudi and J. Kim, *Nature*, **423**, 705 (2003);
    https://doi.org/10.1038/nature01650.
12. S. Kitagawa, R. Kitaura and S. Noro, *Angew. Chem. Int. Ed.*, **43**, 2334 (2004);
    https://doi.org/10.1002/anie.200300610.
13. G. Ferey, C. Mellot-Draznieks, C. Serre and F. Millange, *Acc. Chem. Res.*, **38**, 217 (2005);
    https://doi.org/10.1021/ar040163i.
14. S. Takamizawa, T. Akatsuka and T. Ueda, *Angew. Chem. Int. Ed.*, **47**, 1689 (2008);
    https://doi.org/10.1002/anie.200702950.
15. D.N. Sears, R.E. Wasylishen and T. Ueda, *J. Phys. Chem. B*, **110**, 11120 (2006);
    https://doi.org/10.1021/jp061655a.
16. N. Ohta, A. Fuyuhiro and K. Yamanari, *Chem. Commun.*, **46**, 3535 (2010);
    https://doi.org/10.1039/B923824G.
17. C.Y. Yue, X.W. Lei, Y.X. Ma, N. Sheng, Y.D. Yang, G.D. Liu and X.R. Zhai, *Cryst. Growth Des.*, **14**, 101 (2014);
    https://doi.org/10.1021/cg401208p.
18. H.L. Zhu and X.M. Chen, *Acta Crystallogr. C*, **55**, 2010 (1999);
    https://doi.org/10.1107/S0108270199010525.
19. D. Eisenberg and W. Kauzmann, The Structure and Properties of Water; Oxford University Press: New York (1969).